Carbohydrate Polymers 92 (2013) 1443–1450

Contents lists available at SciVerse ScienceDirect

Carbohydrate Polymers

journal homepage: www.elsevier.com/locate/carbpol

Stability and solubility enhancement of ellagic acid in cellulose ester solid dispersions

Bin Li[a], Kim Harich[b], Lindsay Wegiel[c], Lynne S. Taylor[c], Kevin J. Edgar[a,*]

[a] Department of Sustainable Biomaterials, Virginia Tech, Blacksburg, VA 24061, United States
[b] Department of Biochemistry, Virginia Tech, Blacksburg, VA 24061, United States
[c] Department of Industrial and Physical Pharmacy, College of Pharmacy, Purdue University, West Lafayette, IN 47907, United States

ARTICLE INFO

Article history:
Received 11 September 2012
Received in revised form 19 October 2012
Accepted 22 October 2012
Available online 29 October 2012

Keywords:
Ellagic acid
Amorphous solid dispersion
CMCAB
HPMCAS
CAAdP
Cellulose acetate adipate propionate
PVP
Dissolution
Stability
Bioavailability

ABSTRACT

Structurally varied, carboxyl-containing cellulose derivatives were evaluated for their ability to form amorphous solid dispersions (ASD) with ellagic acid (EA), in order to improve the solubility of this high-melting, poorly bioavailable, but highly bioactive natural flavonoid compound. ASDs of EA with carboxymethylcellulose acetate butyrate (CMCAB), cellulose acetate adipate propionate (CAAdP), and hydroxypropylmethylcellulose acetate succinate (HPMCAS) were prepared, and EA dissolution from these ASDs was compared with that from pure crystalline EA and from EA/poly(vinylpyrrolidinone) (PVP) solid dispersions (SD). Polymer/drug mixtures were characterized by powder X-ray diffraction (XRPD), modulated differential scanning calorimetry (MDSC), nuclear magnetic resonance (NMR) and Fourier transform infrared spectroscopy (FT-IR). The XRPD and FT-IR results indicated that EA was amorphous in solid dispersions with EA concentration up to 25 wt%. The stability against crystallization and solution concentrations of EA from these solid dispersions were significantly higher than those observed for physical mixtures and pure crystalline EA. HPMCAS stabilized EA most effectively, among the polymers tested, against both chemical degradation and recrystallization. The relative ability to solubilize EA from ASDs at pH 6.8 was PVP ≫ HPMCAS ≫ CMCAB. EA dissolves from ASD in PVP quickly and completely (maximum 92%) at pH 6.8, but EA is also released from PVP at pH 1.2, and then crystallizes rapidly. Therefore PVP is not a practical candidate for EA ASD. In contrast, the cellulose derivative ASDs show very slow EA release at pH 1.2 (<4%) and faster but still incomplete drug release at pH 6.8 (maximum 35% for HPMCAS SD). The pH-triggered drug release from HPMCAS ASD makes HPMCAS a practical choice for EA solubility enhancement.

1. Introduction

Ellagic acid is a polyphenolic flavonoid present in many dietary sources including walnuts, pomegranates, strawberries, blackberries, cloudberries and raspberries (Häkkinen, Kärenlampi, Mykkänen, Heinonen, & Törrönen, 2000). It has been found that EA has important beneficial health effects against many oxidation-linked chronic diseases (Landete, 2011; Vattem & Shetty, 2005). Among the most important examples are cancer (including that of the breast (Wang et al., 2012), prostate (Bell & Hawthorne, 2008), lung (Boukharta, Jalbert, & Castonguay, 1992) and colon (González-Sarrías, Espín, Tomás-Barberán, & García-Conesa, 2009), cardiovascular disease (Larrosa, García-Conesa, Espín, & Tomás-Barberán, 2010) and neurodegenerative diseases (Porat, Abramowitz, & Gazit, 2006). However, the poor oral bioavailability of ellagic acid is a great challenge for the study of its beneficial functions, making it difficult to translate in vitro results into in vivo studies. In addition, it has been estimated that the average individual consumes approximately 343 mg EA per year, which is not enough to reach the plasma levels required for lung cancer prevention, given its low bioavailability (Castonguay, Boukharta, & Teel, 1998). Poor EA aqueous solubility (9.3 μg/ml at pH 7.4) (Bala, Bhardwaj, Hariharan, Kharade, et al. 2006; Bala, Bhardwaj, Hariharan, & Kumar, 2006) is a primary cause for its low bioavailability. This low solubility is due in part to its high degree of crystallinity (melting point not observed due to decomposition at ca. 360 °C), which is a direct result of the planar and symmetrical EA structure and the extensive hydrogen-bonding (H-bonding) network formed in the crystal.

In order to develop its therapeutic potential, it is necessary to develop delivery systems that enhance EA solubility, stability and bioavailability. The Bala group developed EA-loaded poly(D,L-lactide-co-glycolide) (PLGA) nanoparticles for oral administration (Bala, Bhardwaj, Hariharan, Kharade, et al. 2006; Bala, Bhardwaj,

* Corresponding author.
E-mail address: kjedgar@vt.edu (K.J. Edgar).

0144-8617/$ – see front matter © 2012 Elsevier Ltd. All rights reserved.
http://dx.doi.org/10.1016/j.carbpol.2012.10.051

Hariharan, & Kumar, 2006). Other investigators studied encapsulation of EA into PLGA and polycaprolactone (PCL) nanoparticles to improve oral bioavailability (Sonaje et al., 2007). There are only a couple of brief reports on complexation of EA with cyclodextrin derivatives to enhance solubility (Boukharta et al., 1992); importantly, one report hints that these complexes may substantially improve EA bioavailability, providing support for the hypothesis that improvement in EA solubility is a viable route for enhancing its oral bioavailability (Chudasama, Lugea, Lu, & Pandol, 2011).

Molecular dispersion in polymer matrices (amorphous solid dispersion, ASD) is a very attractive way to improve the oral bioavailability of drugs with poor water solubility (Konno, Handa, Alonzo, & Taylor, 2008; Qian, Huang, & Hussain, 2010). Low aqueous solubility can be caused in part by high crystallinity, particularly with high-melting drugs like EA. There is therefore reason to believe that trapping EA in the metastable amorphous state in a polymer matrix would effectively enhance its bioavailability. Solid dispersions of drug in polymer may be prepared from a solution in a common solvent (spray-drying, freeze-drying, rotary evaporation, co-precipitation, and film casting), or by co-extrusion. Frequently employed matrix polymers include the water-soluble PVP, and water-swellable and/or dispersible polymers like cellulose acetate phthalate (CAPhth) (DiNunzio, Miller, Yang, McGinity, & Williams, 2008), HPMCAS (Friesen et al., 2008), and CMCAB (Posey-Dowty et al., 2007; Shelton et al., 2009). Very recently, the Edgar and Taylor groups have collaborated to design cellulose ω-carboxyalkanoates, including CAAdP, for high performance as crystallization inhibitors (Ilevbare, Liu, Edgar, & Taylor, 2012a; Ilevbare, Liu, Edgar, & Taylor, 2012b) and ASD polymers (Kar, Liu, & Edgar, 2011; Liu, Kar, & Edgar, 2012). Carboxylated cellulose derivatives are attractive candidate matrices due to their generally benign toxicity profiles, high glass transition temperatures (T_g) and the ability of the pendent carboxyl group to trigger pH-responsive drug release and create strong interactions with hydrogen bonding groups on the drug. Despite the apparent potential of the ASD approach, there have been no reports to date on enhancement of EA solubility in this way.

In order to design effective ASD delivery systems, it is necessary to identify polymers and drug–polymer ratios that meet several key criteria. The drug must be amorphous, and stable with regard to crystallization in the solid phase. The drug must be released under gastrointestinal (GI) conditions at supersaturated concentrations. Released drug must be stabilized by the polymer in solution against crystallization, even under these supersaturated concentrations; this implies that the polymer must have adequate aqueous solubility (at least in the μg/mL range). Herein we report evaluation of EA ASDs with three structurally diverse cellulose derivatives; the somewhat hydrophilic HPMCAS, the rather hydrophobic CMCAB, and the very hydrophobic CAAdP, with respect to their ability to meet these criteria and provide effective solubility enhancement. Our hypothesis is that evaluation of the structure-property relationships will enable us to select or design a polymer that holds the promise of bioavailability enhancement for this important, therapeutically promising flavonoid.

2. Experimental

2.1. Chemicals

Ellagic acid dihydrate (97%) was purchased from Alfa Aesar (Ward Hill, MA). PVP (K29-32, Mw 58,000) and potassium bromide (99+%, for spectroscopy, IR grade) was supplied by Acros Organics (Geel, Belgium). CMCAB (641-0.2) was obtained from Eastman Chemical. CAAdP (DS(acetyl) = 0.04, DS(propionyl) = 2.09, DS(adipate) = 0.33) was synthesized by procedures previously described by us (Kar et al., 2011). HPMCAS (AS-LG) was supplied by Shin-Etsu Chemical Co., Ltd. (Tokyo, Japan). Acetone (HPLC grade, 0.2 μm filtered), reagent ethanol, potassium phosphate monobasic, and sodium hydroxide were supplied by Fisher Scientific (Fair Lawn, NJ). Buffer solutions (pH 6.8 and 1.2) were prepared according to USP30-NF25 standard method.

2.2. Preparation of solid dispersions

2.2.1. Spray-dried solid dispersions

Mixtures of EA/polymer (PVP, CMCAB and HPMCAS) (10.0 g) at different weight ratios (1/9 and 1/3) were dissolved in 500 mL of acetone/ethanol (1/4, v/v) to make feed solutions. Solid dispersions were prepared using a Buchi mini-spray dryer B-290. Operating parameters were: inlet temperature, 90 °C; outlet temperature, 57–60 °C; feed rate, 9 mL/min; nitrogen flow 350 L/h. Yields of the spray-drying process were 50–60%.

2.2.2. Co-precipitated solid dispersions

It was convenient to prepare EA/CAAdP dispersions by co-precipitation due to the limited quantity of CAAdP available, and the unavoidable losses incurred when spray-drying small quantities of solid dispersions. A mixture of EA/CAAdP (1/3 or 1/9) (0.2 g) was dissolved in 10 mL of THF. Then the solution was added dropwise to 200 mL of DI water with stirring. The precipitate was collected by filtration, then dried under vacuum at 40 °C overnight. The drug content was confirmed by UV–vis spectrometry.

2.2.3. ASD by rotary evaporation

It was convenient to prepare the EA/PVP/CAAdP dispersion by rotary evaporation due to the limited quantities of CAAdP available and the high water solubility of PVP. EA (20 mg), PVP (90 mg) and CAAdP (90 mg) were dissolved in acetonitrile/EtOH (1/1, v/v; 40 mL). The solution was concentrated by rotary evaporation. The residue was dried under vacuum at 40 °C overnight.

Physical mixtures were prepared to compare to the spray-dried samples by grinding weighed portions of EA and HPMCAS, CAAdP, CMCAB or PVP with a mortar and pestle.

2.3. Characterization of EA/matrix solid dispersions

EA/polymer solid dispersions were characterized by comparing IR and NMR spectra, DSC traces, and XRPD patterns obtained for EA, the pure individual polymers, physical mixtures of EA/polymer, and EA/polymer solid dispersions.

2.4. IR spectroscopy

IR spectra were recorded in a frequency range between 4000 and 400 cm^{-1}, using a resolution of 4 cm^{-1} and 40 accumulations, on a Nicolet 8700 FT-IR spectrometer. FTIR pellets comprised 1 mg of the polymer matrix mixture and 100 mg of potassium bromide.

2.5. NMR spectroscopy

Solid-state CP MAS ^{13}C-NMR experiments were performed on a BRUKER Avance II 300 spectrometer at 75.47 MHz, equipped with a MAS probe head using 4 mm ZrO_2 rotors. Glycine was used to set the Hartmann–Hahn conditions and adamantane as secondary chemical shift reference δ = 38.48 ppm and 29.46 ppm from external TMS, respectively. Solution ^{13}C-NMR spectra were recorded with a proton 90° pulse length of 4.0 μs and a contact time of 1 ms. Repetition delay was 10 s, spin rate 7k, number of scans 512 within 1.5 h, and spectral width 25 kHz. FIDs were accumulated with a time domain size of 1 K data points. RAMP shape pulse was used during the

cross-polarization and spinal64 for decoupling during acquisition. Spectral data were processed using the Topspin program.

2.6. XRPD analysis

XRPD measurements used a Bruker D8 Discovery X-ray diffractometer. Measurements were performed at a voltage of 40 kV and 25 mA. The scanned angle was set as $5 < 2\theta < 40^\circ$ and the scan rate was 2°/min.

2.7. DSC measurement

EA and solid dispersions were analyzed using a modulated differential scanning calorimeter (Model Q2000, TA Instruments, New Castle, Delaware) equipped with a refrigerated cooling accessory. Samples (4–5 mg) were packed in non-hermetically crimped aluminum pans, heated under dry nitrogen from 25 to 100–120 °C at 10 °C/min to eliminate moisture and relieve stress, then quickly cooled to 25 °C at 100 °C/min. Samples were then heated to 200 °C at 3 °C/min with ±1 °C modulation every 45 s; glass transitions are reported from this second heating scan based on the reversible heat flow. DSC heating curves were analyzed using Universal Analysis 2000 software (TA Instruments).

2.8. UV–vis spectroscopy

All UV–vis spectra were recorded on a Thermo Scientific Evolution 300 UV-Visible Spectrometer.

2.9. Measurement of matrix polymer solubility

Polymer (0.5 g; CMCAB, HPMCAS, CAAdP, or PVP) was dispersed in 10 mL of pH 6.8 buffer. The suspension was mixed by a vortex mixer for 1 min, ultrasonicated for 15 min, and then shaken for 24 h at room temperature (Burrell wrist action shaker, Model 75). The suspension/solution was centrifuged at 14,000 × *g* for 10 min to remove insoluble material. An aliquot (1 mL) of the top, clear solution was withdrawn and the solvent evaporated in an oven (80 °C, 5 h). The dissolved polymer weight was calculated by subtracting the weight of salt in buffer solution (7.2 ± 0.1 mg/mL). The dissolved polymer concentration (w/v) was then calculated by dividing the dissolved polymer weight by the volume of solution withdrawn.

2.10. Ellagic acid calibration curves in N-methylpyrrolidone (NMP) and pH 6.8 buffer

2.10.1. EA calibration curve

Careful attention is needed in construction of a practical and appropriate calibration curve that covers supersaturated concentrations of a poorly soluble species like EA. From the standard curves of EA (see Supplementary Material S3), the extinction coefficient of EA is quite similar in NMP (38.3 $L\,g^{-1}\,cm^{-1}$) and in NMP/pH 6.8 buffer solution (1/99, v/v; 39.5 $L\,g^{-1}\,cm^{-1}$). In creating appropriate calibration curves, one must also keep in mind the ionization state of a molecule like EA that possesses multiple weakly acidic phenol groups (Hasegawa et al., 2003). We used EA UV/vis calibration curves in NMP for experiments at pH 1.2, and calibration curves in NMP/pH 6.8 buffer (1/99, v/v) for experiments at pH 6.8.

The EA standard curve in NMP was used for the calculation of concentration from UV–vis absorption at pH 1.2 since most EA is not ionized at that pH. Calibration curves in aqueous buffer (pH 6.8) were generated by dilution of an EA stock solution in NMP (2.5 mg/mL) with pH 6.8 buffer solution to 10 mL (fixing the ratio of NMP/pH 6.8 buffer 1/99, v/v).

2.10.2. Dissolution testing

EA solid dispersion (EA content fixed at 50 mg) was dispersed in 10 mL of pH 6.8 phosphate buffer in an amber flask with magnetic stirring for 24 h. Then the suspension was centrifuged (14,000 × *g*, 10 min) to remove insoluble material. EA concentration in the supernatant was determined by UV–vis spectrometry using the calibration curve in pH 6.8 buffer generated as described above.

2.10.3. Enhancement of ellagic acid stability

Stability enhancement of EA by polymers in solution was studied by following decline in EA solution concentration in the presence or absence of polymer, using UV–vis spectrometry. EA and EA/PVP (1/9) solid dispersion samples were dissolved in ethanol, while EA/cellulose ester (1/9) solid dispersions were dissolved in THF due to the low solubility of cellulose derivatives in ethanol. EA concentration was fixed at 0.2 mg/mL. Samples (1 mL) of each stock solution were diluted to 10 mL with pH 6.8 buffer. The amount of EA still in solution was measured by UV–vis absorption of the diluted solution at time intervals from 0.5 to 24 h.

EA chemical degradation in aqueous buffer was studied as follows. Samples of EA or EA/polymer 1/9 solid dispersion were dissolved in ethanol or THF ([EA] = 0.2 mg/mL), then 200 μL aliquots of each solution were added to pH 6.8 aqueous buffer (800 μL). Samples were incubated at room temperature for the indicated time. After incubation, each mixture was diluted by 1 mL of ethanol and the UV–vis absorption of the diluted solution was measured.

2.10.4. Ellagic acid release profile

EA samples (pure, physical mixture or solid dispersion) were dispersed in 100 mL pH 6.8 buffer in an amber glass flask in amounts that provided in each case an EA concentration of 0.05 mg/mL. The solution was stirred with a stir bar at 25 °C. Aliquots (1.5 mL) were withdrawn at appropriate time intervals and replaced with 1.5 mL of fresh dissolution medium after each sampling to maintain constant volume. UV–vis absorption of each aliquot was recorded after centrifugation (14,000 × *g*, 10 min). Release profiles in pH 1.2 buffer were measured using the same method and the aliquots were centrifuged before UV–vis measurement. The first three time points (0.1, 1.3, 2.7 min) from EA/PVP 1/9 solid dispersions were measured directly without centrifugation, because of the rapid initial release from those dispersions and the time required for centrifugation.

3. Results and discussion

Symmetrical, planar ellagic acid (Fig. 1) is a highly crystalline compound (Rossi, Erlebacher, Zacharias, Carrell, & Iannucci, 1991). We hypothesized that solid dispersion in polymers with sufficient ability to form H-bonds with its functional groups may stabilize amorphous EA, permitting formation of metastable amorphous EA dispersions with sufficient storage stability. However, it is possible that the dearth of publications about ASD of EA in the literature may be due to concerns about its rapid crystallization either in the solid ASD, or after release into the gastrointestinal lumen. Due to recent success in forming ASDs of the flavonoids curcumin and quercetin using cellulose ester polymers, we chose to take on the daunting challenge of EA. Three cellulose derivatives were of particular interest to us. It has recently been demonstrated that the pH-responsive, hydrophobic CMCAB is an effective ASD polymer, providing rapid release of relatively soluble drugs like aspirin and ibuprofen, and zero-order release of poorly soluble drugs like griseofulvin and glyburide, while substantially increasing solution concentrations of those poorly soluble drugs vs. pure drug (Posey-Dowty et al., 2007; Shelton et al., 2009). HPMCAS was chosen for comparison because of its greater water solubility, and because it has proven to be an effective ASD polymer (Curatolo, Nightingale, & Herbig, 2009) (it is included in several recent New Drug Applications before the

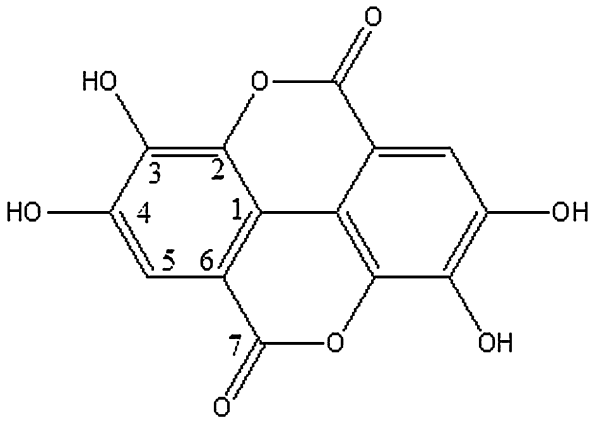

Fig. 1. Chemical structure of ellagic acid.

FDA). Finally we selected CAAdP, which we have recently designed as a highly effective ASD polymer, for evaluation. CAAdP is even more hydrophobic than CMCAB and has low water solubility, but is pH responsive, and interacts strongly with hydrophobic drugs like ritonavir and curcumin. It has been shown to strongly inhibit the crystal growth of ritonavir (Ilevbare et al., 2012b), suggesting that it will prove to be an effective ASD polymer. We compared these polysaccharide derivatives not only with pure EA, but also with the widely used and historically important ASD polymer PVP (Rumondor, Marsac, Stanford, & Taylor, 2009). PVP has quite different characteristics from the cellulosic polymers, being rather water soluble, even at low pH (due to its slightly basic amide groups). We studied the preparation and characterization of EA/polymer solid dispersions, and their dissolution behavior. We hypothesized that this set of polymers would provide deep insight into the structure/property/functional relationships of EA dispersions in polymer matrices, and the impact of those matrices on EA aqueous solution concentrations.

3.1. Characterization of spray dried amorphous solid dispersions

First we studied the ability of each polymer to stabilize against EA crystallization in the solid phase. We prepared solid dispersions of EA/polymer at various weight ratios and compared with pure EA and physical mixtures. Blends were characterized by the following techniques.

XRPD was used to investigate room temperature crystallinity of the EA/polymer blends. XRPD patterns (Fig. 2 and S1) of all EA/polymer solid dispersions showed halo patterns without EA diffraction peaks, similar to those of the corresponding pure polymers, except for EA/CMCAB 1/3 and EA/CAAdP 1/3 solid dispersions, where small peaks at 28° and 12° indicated that EA was not completely amorphous at this ratio with these polysaccharides. These results indicate that EA solid dispersions in HPMCAS and PVP are amorphous up to 25 wt% EA, and up to 10% EA in CMCAB and CAAdP.

DSC can provide information about both polymer and drug properties, over a wide range of temperatures. DSC analysis temperatures for dispersions containing CAAdP, CMCAB and HPMCAS were kept below 200 °C, since these polymers undergo crosslinking esterification reactions between the pendent carboxyl and hydroxyl groups above 200 °C. Modulated DSC was an effective method for determining T_g values based on reversible heat flows (Supporting Material S2). DSC second heating curves of amorphous EA solid dispersions as well as those of pure EA and the individual matrix polymers are shown in Fig. 3(A–C), and the T_g values of EA solid dispersions are plotted vs. EA content in Fig. 3(D). T_g values of polymers in EA ASDs decreased compared to those of the corresponding pure polymers. Interestingly, T_g decreases with increasing EA content in CMCAB, but not in PVP or HPMCAS matrices. Increasing EA concentration in HPMCAS has little effect on T_g, while in PVP matrices, increasing EA concentration actually seems to have an anti-plasticization effect. The failure of the PVP/EA blends to obey a Gordon–Taylor type relationship, in spite of strong XRD and DSC evidence of miscibility, could be due to strong polymer–drug interactions (Janssens & Van den Mooter, 2009). CAAdP/EA ASDs behave in intermediate fashion, with decreasing Tg up to 1/9 ratio, but then a rise in T_g at higher EA levels (remember that blends above 10% EA in CAAdP are not entirely amorphous).

FTIR is useful for identifying strong polymer-drug interactions. IR spectra of EA, HPMCAS, and EA/HPMCAS (1/1 and 1/3) spray dried solid dispersions are shown in Fig. 4. The EA band at 2800–3700 cm^{-1} was attributed to OH stretching with a broad peak around 3077 cm^{-1} and a small sharp peak at 3558 cm^{-1}, which disappeared in the spectra of solid dispersions. The spray-dried dispersions show a broad OH stretching peak at 3475 cm^{-1} and a strong methylene stretching peak at 2937 cm^{-1}, similar to the bands of pure HPMCAS (3404 and 2937 cm^{-1}). The distinct change in the OH stretching area indicates polymer–EA hydrogen bonding (H-bonding). In addition, the HPMCAS C=O stretching peak at 1739 cm^{-1} shifts slightly to 1741 cm^{-1}. Moreover, the EA C=O stretching peak at 1699 cm^{-1} disappeared. These changes indicate that the carbonyl groups of both HPMCAS and EA are involved in H-bonding interactions.

Solid-state ^{13}C-NMR may provide more evidence about the nature of EA–matrix polymer interactions. CPMAS ^{13}C-NMR spectra of HPMCAS, EA and EA/HPMCAS 1/3 solid dispersion are shown in Fig. 5. The EA spectrum was assigned following the literature (Li, Elsohly, Hufford, & Clark, 1999). EA peaks are located between 105 and 165 ppm and do not overlap with HPMCAS peaks. Therefore, changes of peak shapes and/or shifts of EA carbons in ASDs

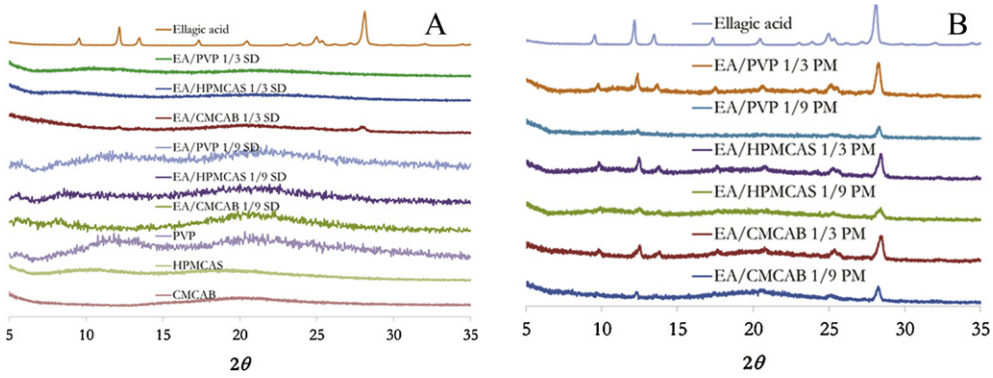

Fig. 2. XRPD patterns of (A) EA, PVP, HPMCAS, CMCAB and EA/polymer spray dried solid dispersions; (B) EA and EA/polymer physical mixtures.

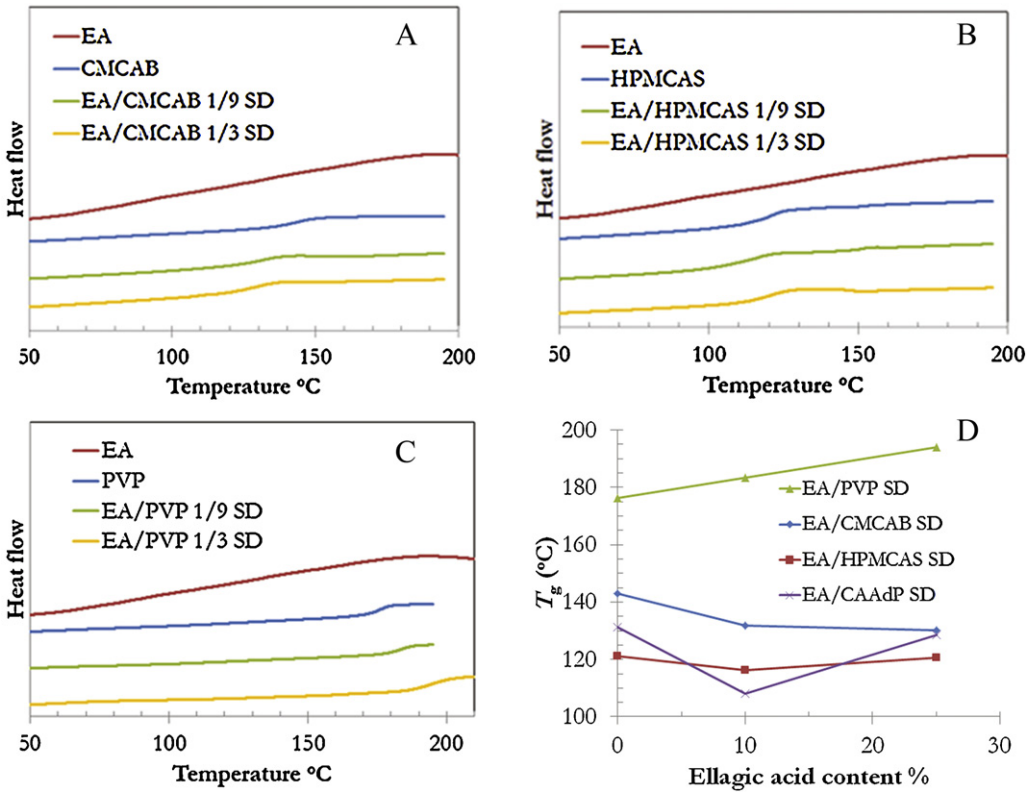

Fig. 3. (A) MDSC heating curves of EA, CMCAB and EA/CMCAB solid dispersions; (B) MDSC heating curves of EA, HPMCAS and EA/HPMCAS solid dispersions; (C) DSC heating curves of EA, PVP and EA/PVP solid dispersions; (D) T_g values of EA solid dispersions vs. EA content.

are diagnostic of H-bonding between EA and polymer matrices. We found that in the solid dispersion spectrum all of the EA peaks were broadened. Some peaks combined to form broad peaks, for instance, C1, C5 and C6; and C2 and C3. Chemical shifts of some peaks changed slightly, for example, C7 (from 161.4 ppm in EA to 159.7 ppm in EA/HPMCAS 1/3 SD) and C4 (from 146.5 ppm in EA to 147.6 ppm in EA/HPMCAS 1/3 SD). These peak shape and chemical shift changes confirmed H-bonding interactions between EA and the polymer matrices.

3.2. Suppression of ellagic acid degradation

Stability of ellagic acid in pH 6.8 aqueous buffer has been little studied. In their deprotonation study, Hasegawa et al. found that the EA UV–vis spectrum changed dramatically at pH >12.4, which was explained by opening of the lactone ring (Hasegawa et al., 2003). Other flavonoids have been shown to undergo photochemical, radical, and retro-aldol decomposition reactions under relatively mild conditions (Wang et al., 1997; Zenkevich et al., 2007; Zheng, Haworth, Zuo, Chow, & Chow, 2005).

UV–vis spectrometry was used to study EA chemical stability at pH 6.8. After incubation of EA at pH 6.8 for various time periods, samples were diluted with ethanol to dissolve any solids present; this was so that we could evaluate chemical degradation separately from EA crystallization. The results (Fig. 6(A)) show that the degradation loss of pure EA is 20% after incubation at pH 6.8 for 24 h.

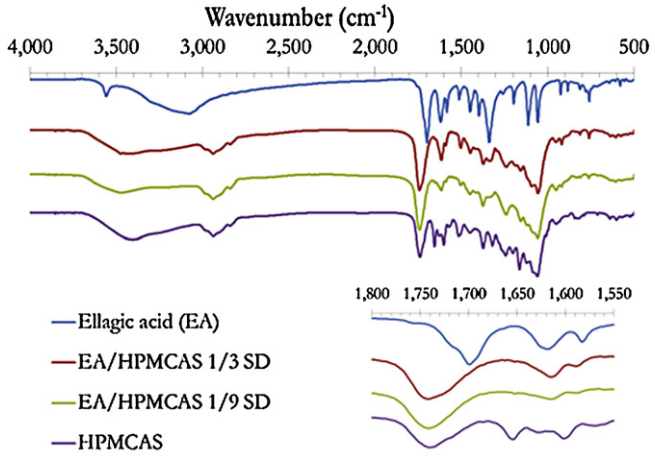

Fig. 4. FTIR spectra of EA, HPMCAS and EA/HPMCAS solid dispersions.

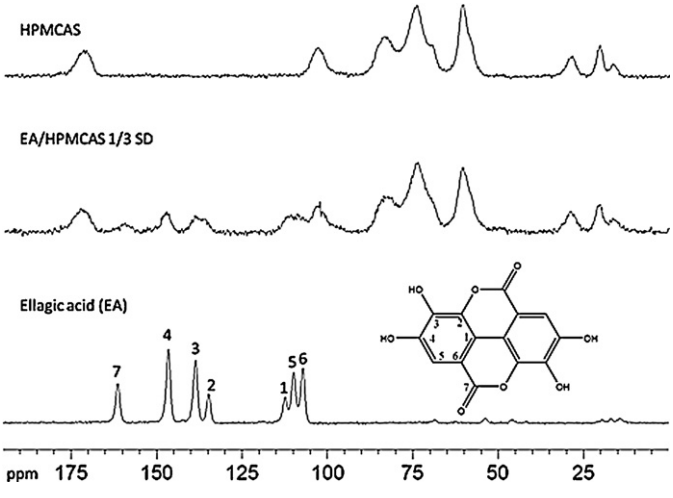

Fig. 5. Solid-State CPMAS ^{13}C-NMR spectra of HPMCAS, EA and EA/HPMCAS 1/3 solid dispersion.

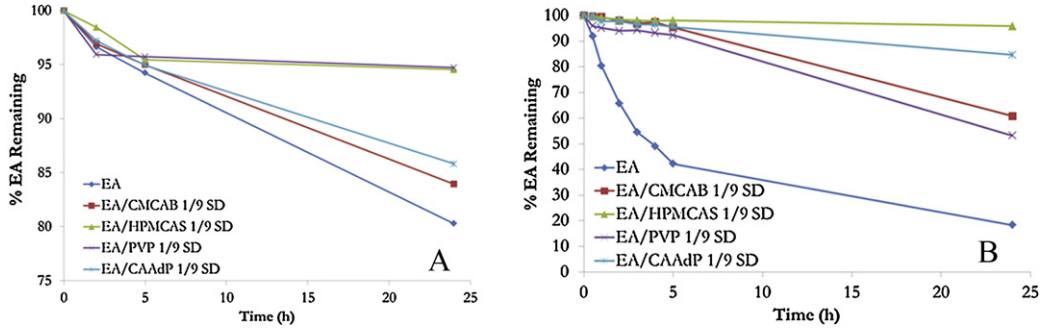

Fig. 6. (A) Stability of EA and EA/polymer solid dispersions in 6.8 buffer (UV–vis after EtOH dilution); (B) stability of EA and EA/polymer solid dispersions in pH 6.8 buffer (UV–vis, no EtOH added).

In contrast, EA in spray dried solid dispersions (EA/polymer 1/9) is protected from degradation to an extent dependent on polymer structure; EA degradation in ASDs was 16% (CMCAB), 14% (CAAdP), 6% (PVP), and 5% (HPMCAS). Protection against degradation is better in more hydrophilic polymer matrices; this would be consistent with a degradation mechanism involving hydrophobic dioxygen (Priyadarsini, Khopde, Kumar, & Mohan, 2002).

In order to evaluate the effectiveness of each polymer in producing stable, supersaturated EA solutions in the small intestine, we evaluated stability against crystallization in pH 6.8 buffer. We incubated ASD samples and pure EA at pH 6.8 and room temperature, this time without ethanol dilution prior to UV–vis measurement. The results show the combined effects of EA crystallization and degradation (Fig. 6(B)). Pure EA was removed from solution rapidly, only 42% remaining in solution after 5 h and only 18% after 24 h. Loss of dissolved EA is primarily due to EA crystallization, since only about 20% EA chemical degradation was experienced over 24 h under identical conditions. In contrast, after 24 h 95% of EA remained in solution from HPMCAS solid dispersion, vs. 85%, 61% and 53% for CAAdP, CMCAB and PVP ASDs, respectively. HPMCAS ASDs provided effective stabilization against both EA crystallization and chemical degradation.

3.3. Dissolution testing and solution concentration enhancement

Maximum solution concentration from pure EA and its ASDs at pH 6.8 was measured by UV–vis spectrometry. Such studies can be plagued by UV absorption by nanoparticles that can result from partial crystallization from such supersaturated solutions. We dealt with this issue by centrifugation of samples prior to UV–vis measurements. This protocol gave highly repeatable values with a standard deviation of less than 5% for three duplicates. In the dissolution tests, EA solid dispersions were dispersed in pH 6.8 buffer solution. Aliquots were removed, centrifuged and analyzed at various time points (Supporting Material Fig. S4). Equilibrium was usually reached (as determined by [EA] plateau) within 1–5 h. PVP and HPMCAS molecular dispersions with lower EA content led to higher EA solution concentrations, in accord with the pioneering work by Higuchi et al. (Simonelli, Mehta, & Higuchi, 1969; Simonelli, Mehta, & Higuchi, 1976). EA solution concentration obtained from solid dispersions depends strongly on polymer structure in the following sequence PVP > HPMCAS > CMCAB, which corresponds with the relative aqueous solubility of the three polymers (Table 1). This relationship may be a result of the fact that more hydrophilic polymer matrices swell or dissolve more rapidly in aqueous buffer, affording faster release kinetics. Increased EA solution concentration could also result from the higher polymer solution concentrations observed with PVP and HPMCAS; the increased amounts of dissolved polymer may increase thermodynamic solubility of EA, or may more effectively inhibit EA crystallization and degradation. It should be noted that very recently, an interesting study has appeared illustrating that higher thermodynamic solubility (for example, by cyclodextrin complexation) may actually slow down permeation of a drug from the GI lumen to the bloodstream (Miller, Beig, Carr, Spence, & Dahan, 2012).

3.4. Drug release profiles

Dissolution of EA from ASDs was compared with that of pure EA (5 mg) and that from EA/polymer physical mixtures, both at pH 6.8 and 1.2. Nanoparticle removal from sample aliquots was effected by centrifugation (14,000 × *g*). UV–vis absorption of the solution was measured and plotted vs. time. The influence of polymer type and of EA/polymer ratio on drug release profiles was also investigated.

Drug release profiles of EA, EA/PVP 1/9 physical mixture, and EA/polymer (CMCAB, CAAdP, HPMCAS and PVP) ASDs in pH 6.8 buffer are shown in Fig 9. Release from the EA/PVP 1/9 solid dispersion was fastest and most complete (Fig. 7(A)), reaching 92% within 1 h, while release from the EA/HPMCAS blend (1/9 SD) was much slower and incomplete, reaching a maximum of 35% after 0.5 h. Release from the EA/CMCAB 1/9 SD was slowest, reaching a maximum of 18% after 1 h. EA concentration in each case decreased from a maximum value, presumably due to incomplete stabilization of supersaturated EA concentrations by the polymers. After 24 h, the drug release yield from EA/PVP and EA/HPMCAS 1/9 SDs decreased to 13–14%, and from EA/CMCAB 1/9 SD was only 6%. Release from the EA/PVP 1/9 physical mixture was much slower and less complete than that from the ASD of the same composition, reaching a maximum of 19% EA released at 3 h; we see a similar relative comparison of HPMCAS 1/9 ASD with the HPMCAS physical mixture of equal composition. After 24 h the amount of EA in solution from PVP 1/9 ASD and physical mixture is the same; clearly at long dissolution times the recrystallization of EA, and the failure of these polymers to completely prevent it, becomes an important factor. However the higher extent of release from PVP ASD in the early part of the curve means that there would be much more chance of EA absorption, and presumably much higher bioavailability, from the ASD than from the physical mixture. Dissolution from both PVP and HPMCAS ASDs is far superior to that of pure EA, which reaches

Table 1
Solubility of polymers and maximum EA concentration from their ASDs.

Polymer	Solubility in water (mg/mL)	Maximum EA concentration from amorphous dispersion (μg/mL)
PVP	>600	1500
HPMCAS	23.4	280
CMCAB	1.6	30
CAAdP	1.5	Not measured

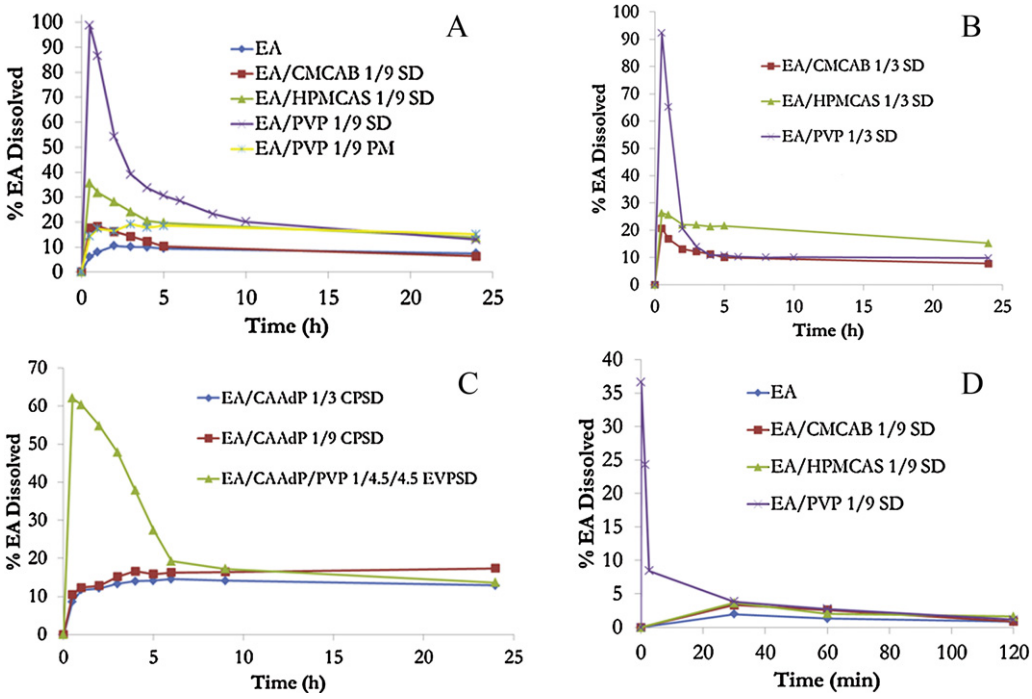

Fig. 7. Dissolution from (A) EA, EA/PVP 1/9 physical mixture, EA/polymer 1/9 solid dispersions (pH 6.8, UV–vis); (B) EA/polymer 1/3 solid dispersions (pH 6.8, UV–vis) (C) EA/CAAdP (1/3, 1/9) co-precipitating solid dispersions (CPSD) and EA/CAAdP/PVP (1/4.5/4.5) evaporation solid dispersion (EVSD), after centrifugation at 14,000 × *g* for 10 min (pH 6.8, UV–vis); (D) dissolution of EA and EA/polymer 1/9 ASDs (pH 1.2, UV–vis).

a maximum of 11% at 2 h, then decreases to 7% at 24 h. Dissolution from the CMCAB ASDs is slow, similar to that from pure EA; we believe that this is due largely to poor release of hydrophobic EA from the hydrophobic CMCAB matrix. This analysis is supported by the reasonable ability of CMCAB to stabilize EA against crystallization and degradation once it is in solution (Fig. 6(B)). Overall we see that supersaturated solutions of EA can be achieved from HPMCAS and PVP ASDs, but that even these polymers retard, but do not stop crystallization of the highly symmetrical EA from supersaturated solutions.

EA/polymer ratio is an important factor impacting extent of drug release. Release from EA/PVP 1/3 ASDs (Fig. 7(B)) reaches a maximum of 76%, decreasing rapidly to 17% within 2 h. Compared with the release profile from EA/PVP 1/9 SD (Fig. 7(A)), the 1/3 ASD affords lower maximum EA release and much faster decrease in EA concentration after the peak. Thus the release rate and the inhibition of EA crystallization strongly depend on the concentration of the PVP ASD. The slower drug release from EA/HPMCAS and EA/CMCAB 1/3 and 1/9 ASDs appears to be somewhat less dependent on EA concentration in the ASD.

CAAdP solid dispersions show drug release profiles similar to those of pure EA and EA/PVP 1/9 PM (Fig. 7(C)). The highest drug release from CAAdP ASDs is around 15–17%, similar to that of CMCAB ASDs. Since CAAdP and CMCAB have similar solubility in pH 6.8 aqueous buffer, it is not surprising that their ASDs show similar drug release profiles. To improve CAAdP drug release properties, an interesting experiment was conducted in which a combination of PVP and CAAdP (1/1, w/w) was used to prepare an ASD blend with 10% EA content by rotary evaporation. The release profile of EA/CAAdP/PVP (1/4.5/4.5) ASD is similar to EA/PVP 1/9 ASD except that the maximum release at 0.5 h is somewhat lower (62%). EA release from 1 to 5 h is higher than that from EA/PVP 1/3 SD, but lower than that from EA/PVP 1/9 SD, which is reasonable since the EA/PVP ratio is 1/4.5 in this solid dispersion. This experiment highlights the potential of properly designed ASD polymer blends for achieving all requirements of a functional ASD formulation.

It was enlightening to compare EA release from these solid dispersions under conditions similar to those of the stomach, in pH 1.2 buffer (Fig. 7(D)). Release from the PVP amorphous blend (EA/PVP 1/9 SD) was quite fast but the percentage of dissolved EA decreased very quickly, reaching 37% within a few seconds (the peak release is so early and decline from the peak is so rapid that it is difficult to sample quickly enough; the actual peak could be even higher). In contrast, release was very slow from EA amorphous dispersions with CMCAB and HPMCAS. These results are perfectly consistent with the slightly basic nature of PVP and the acidic nature of the carboxyl-containing cellulose esters. Low pH release from the three cellulose ester ASDs is minimal and similar to that from pure EA and from the physical mixtures. In contrast, a substantial portion of EA is released from the PVP ASD, then recrystallizes at pH 1.2. This suggests that although EA/PVP 1/9 ASD affords the best EA release at pH 6.8 among the ASDs studied, this advantage would not be observed in the human GI tract. EA would be largely released and recrystallized in the stomach, and would no longer be part of an ASD by the time it reached the small intestine. In contrast, the cellulose derivatives can retain EA in the amorphous dispersion in the stomach, and HPMCAS 1/9 ASD would provide effective drug release in the small intestine.

4. Conclusions

Ellagic acid and the polymers PVP, CAAdP, CMCAB, and HPMCAS were readily blended by spray-drying, affording amorphous solid dispersions with EA content up to 25%. Release from dispersions in pure CAAdP or CMCAB at pH 6.8 was very slow and did not achieve adequate EA dissolution. Although release from the 1/9 ASD with the more soluble HPMCAS was slower and less complete in comparison with that from a 1/9 PVP ASD, HPMCAS matrices show the most promise for EA release, due to rapid EA release and recrystallization observed at gastric pH from PVP ASDs. In addition, HPMCAS amorphous dispersions show excellent ability to inhibit EA crystallization and degradation in solution. Within

this group of polymers, all were capable of stabilizing ellagic acid in the solid phase (as indicated by DSC and PXRD results), but only the more water-soluble polymers (PVP and HPMCAS) afforded very high solution concentrations. Comparison of maximum solution concentration data and solution stabilization data makes it clear that the major impact of polymer hydrophilicity is upon dissolution rate, rather than on stabilization against crystallization from solution. Design of ASD polymers that retain the ability to stabilize EA against crystallization from solid and solution phases displayed by, for example, CAAdP, but with higher water solubility and thus release rate, would be desirable for maximizing EA solution concentrations.

We conclude therefore that HPMCAS is a practical and promising matrix for EA amorphous solid dispersion, stabilization, solubilization, and bioavailability enhancement. We have further shown that blending of ASD polymers with complementary properties can afford functional ASD dispersions that perform better than those based on any individual polymer. Systems based on these solid dispersions provide a promising way to evaluate the efficacy and dosage requirements of EA-based therapeutic and dietary supplement formulations, and potentially to effectively deliver EA to patients.

Acknowledgements

We thank USDA (Grant number 09-35603-05068) for financial support and the Virginia Tech Institute for Critical Technologies and Applied Science (ICTAS) for their support of this project. We thank Eastman Chemical Company and Shin-Etsu, Ltd. for their gracious donations of CMCAB and HPMCAS, respectively.

Appendix A. Supplementary data

Supplementary data associated with this article can be found, in the online version, at doi:10.1016/j.carbpol.2012.10.051.

References

Bala, I., Bhardwaj, V., Hariharan, S., Kharade, S. V., Roy, N., & Ravi Kumar, M. N. V. (2006). Sustained release nanoparticulate formulation containing antioxidant–ellagic acid as potential prophylaxis system for oral administration. *Journal of Drug Targeting*, *14*, 27–34.

Bala, I., Bhardwaj, V., Hariharan, S., & Kumar, M. N. V. R. (2006). Analytical methods for assay of ellagic acid and its solubility studies. *Journal of Pharmaceutical and Biomedical Analysis*, *40*, 206–210.

Bell, C., & Hawthorne, S. (2008). Ellagic acid, pomegranate and prostate cancer—a mini review. *Journal of Pharmacy and Pharmacology*, *60*, 139–144.

Boukharta, M., Jalbert, G., & Castonguay, A. (1992). Biodistribution of ellagic acid and dose-related inhibition of lung tumorigenesis in A/J mice. *Nutrition and Cancer*, *18*, 181–189.

Castonguay, A., Boukharta, M., & Teel, R. (1998). Biodistribution of, antimutagenic efficacies in *Salmonella typhimurium* of, and inhibition of P450 activities by ellagic acid and one analogue. *Chemical Research in Toxicology*, *11*, 1258–1264.

Chudasama, Y. N., Lugea, A., Lu, Q. Y., & Pandol, S. J. (2011). Beta-cyclodextrin increases bioavailability of ellagic acid in rats. *Gastroenterology*, *140*, S-S860.

Curatolo, W., Nightingale, J., & Herbig, S. (2009). Utility of hydroxypropylmethylcellulose acetate succinate (HPMCAS) for initiation and maintenance of drug supersaturation in the GI milieu. *Pharmaceutical Research*, *26*, 1419–1431.

DiNunzio, J. C., Miller, D. A., Yang, W., McGinity, J. W., & Williams, R. O., 3rd. (2008). Amorphous compositions using concentration enhancing polymers for improved bioavailability of itraconazole. *Molecular Pharmaceutics*, *5*, 968–980.

Friesen, D. T., Shanker, R., Crew, M., Smithey, D. T., Curatolo, W. J., & Nightingale, J. A. (2008). Hydroxypropyl methylcellulose acetate succinate-based spray-dried dispersions: An overview. *Molecular Pharmaceutics*, *5*, 1003–1019.

González-Sarrías, A., Espín, J.-C., Tomás-Barberán, F. A., & García-Conesa, M.-T. (2009). Gene expression, cell cycle arrest and MAPK signalling regulation in Caco-2 cells exposed to ellagic acid and its metabolites, urolithins. *Molecular Nutrition & Food Research*, *53*, 686–698.

Häkkinen, S. H., Kärenlampi, S. O., Mykkänen, H. M., Heinonen, I. M., & Törrönen, A. R. (2000). Ellagic acid content in berries: Influence of domestic processing and storage. *European Food Research and Technology*, *212*, 75–80.

Hasegawa, M., Terauchi, M., Kikuchi, Y., Nakao, A., Okubo, J., Yoshinaga, T., et al. (2003). Deprotonation processes of ellagic acid in solution and solid states. *Monatshefte fur Chemie*, *134*, 811–821.

Ilevbare, G. A., Liu, H., Edgar, K. J., & Taylor, L. (2012). Inhibition of solution crystal growth of ritonavir by cellulose polymers – Factors influencing polymer effectiveness. *CrystEngComm*, *14*, 6503–6514.

Ilevbare, G. A., Liu, H., Edgar, K. J., & Taylor, L. S. (2012). Understanding Polymer Properties Important for Crystal Growth Inhibition—Impact of Chemically Diverse Polymers on Solution Crystal Growth of Ritonavir. *Crystal Growth and Design*, *12*, 3133–3143.

Janssens, S., & Van den Mooter, G. (2009). Review: Physical chemistry of solid dispersions. *Journal of Pharmacy and Pharmacology*, *61*, 1571–1586.

Kar, N., Liu, H., & Edgar, K. J. (2011). Synthesis of cellulose adipate derivatives. *Biomacromolecules*, *12*, 1106–1115.

Konno, H., Handa, T., Alonzo, D. E., & Taylor, L. S. (2008). Effect of polymer type on the dissolution profile of amorphous solid dispersions containing felodipine. *European Journal of Pharmaceutics and Biopharmaceutics*, *70*, 493–499.

Landete, J. M. (2011). Ellagitannins, ellagic acid and their derived metabolites: A review about source, metabolism, functions and health. *Food Research International*, *44*, 1150–1160.

Larrosa, M., García-Conesa, M. T., Espín, J. C., & Tomás-Barberán, F. A. (2010). Ellagitannins, ellagic acid and vascular health. *Molecular Aspects of Medicine*, *31*, 513–539.

Li, X.-C., Elsohly, H. N., Hufford, C. D., & Clark, A. M. (1999). NMR assignments of ellagic acid derivatives. *Magnetic Resonance in Chemistry*, *37*, 856–859.

Liu, H., Kar, N., & Edgar, K. (2012). Direct synthesis of cellulose adipate derivatives using adipic anhydride. *Cellulose*, *19*, 1279–1293.

Miller, J. M., Beig, A., Carr, R. A., Spence, J. K., & Dahan, A. (2012). A win–win solution in oral delivery of lipophilic drugs: Supersaturation via amorphous solid dispersions increases apparent solubility without sacrifice of intestinal membrane permeability. *Molecular Pharmaceutics*, *9*, 2009–2016.

Porat, Y., Abramowitz, A., & Gazit, E. (2006). Inhibition of amyloid fibril formation by polyphenols: Structural similarity and aromatic interactions as a common inhibition mechanism. *Chemical Biology & Drug Design*, *67*, 27–37.

Posey-Dowty, J. D., Watterson, T. L., Wilson, A. K., Edgar, K. J., Shelton, M. C., & Lingerfelt, L. R. (2007). Zero-order release formulations using a novel cellulose ester. *Cellulose*, *14*, 73–83.

Priyadarsini, K. I., Khopde, S. M., Kumar, S. S., & Mohan, H. (2002). Free radical studies of ellagic acid, a natural phenolic antioxidant. *Journal of Agricultural and Food Chemistry*, *50*, 2200–2206.

Qian, F., Huang, J., & Hussain, M. A. (2010). Drug–polymer solubility and miscibility: Stability consideration and practical challenges in amorphous solid dispersion development. *Journal of Pharmaceutical Sciences*, *99*, 2941–2947.

Rossi, M., Erlebacher, J., Zacharias, D. E., Carrell, H. L., & Iannucci, B. (1991). The crystal and molecular structure of ellagic acid dihydrate: A dietary anti-cancer agent. *Carcinogenesis*, *12*, 2227–2232.

Rumondor, A. C., Marsac, P. J., Stanford, L. A., & Taylor, L. S. (2009). Phase behavior of poly(vinylpyrrolidone) containing amorphous solid dispersions in the presence of moisture. *Molecular Pharmaceutics*, *6*, 1492–1505.

Shelton, M. C., Posey-Dowty, J. D., Lingerfelt, L. R., Kirk, S. K., Klein, S., & Edgar, K. J. (2009). Enhanced dissolution of poorly soluble drugs from solid dispersions in carboxymethylcellulose acetate butyrate matrices. In K. J. Edgar, T. Heinze, & T. Liebert (Eds.), *Polysaccharide Materials: Performance by Design* (pp. 93–113). Washington, DC: American Chemical Society.

Simonelli, A. P., Mehta, S. C., & Higuchi, W. I. (1969). Dissolution rates of high energy polyvinylpyrrolidone (PVP)-sulfathiazole coprecipitates. *Journal of Pharmaceutical Sciences*, *58*, 538–549.

Simonelli, A. P., Mehta, S. C., & Higuchi, W. I. (1976). Dissolution rates of high energy sulfathiazole–povidone coprecipitates II: Characterization of form of drug controlling its dissolution rate via solubility studies. *Journal of Pharmaceutical Sciences*, *65*, 355–361.

Sonaje, K., Italia, J. L., Sharma, G., Bhardwaj, V., Tikoo, K., & Kumar, M. N. V. R. (2007). Development of biodegradable nanoparticles for oral delivery of ellagic acid and evaluation of their antioxidant efficacy against cyclosporine A-induced nephrotoxicity in rats. *Pharmaceutical Research*, *24*, 899–908.

Vattem, D. A., & Shetty, K. (2005). Biological functionality of ellagic acid: A review. *Journal of Food Biochemistry*, *29*, 234–266.

Wang, N., Wang, Z.-Y., Mo, S.-L., Loo, T., Wang, D.-M., Luo, H.-B., et al. (2012). Ellagic acid, a phenolic compound, exerts anti-angiogenesis effects via VEGFR-2 signaling pathway in breast cancer. *Breast Cancer Research and Treatment*, *134*, 943–955.

Wang, Y.-J., Pan, M.-H., Cheng, A.-L., Lin, L.-I., Ho, Y.-S., Hsieh, C.-Y., et al. (1997). Stability of curcumin in buffer solutions and characterization of its degradation products. *Journal of Pharmaceutical and Biomedical Analysis*, *15*, 1867–1876.

Zenkevich, I. G., Eshchenko, A. Y., Makarova, S. V., Vitenberg, A. G., Dobryakov, Y. G., & Utsal, V. A. (2007). Identification of the products of oxidation of quercetin by air oxygen at ambient temperature. *Molecules*, *12*, 654–672.

Zheng, Y., Haworth, I. S., Zuo, Z., Chow, M. S. S., & Chow, A. H. L. (2005). Physicochemical and structural characterization of quercetin-β-cyclodextrin complexes. *Journal of Pharmaceutical Sciences*, *94*, 1079–1089.